ISSN 1870-4069

Evaluation of Breast Cancer by Infrared Thermography

Antony Morales Cervantes[1] , Eleazar Samuel Kolosovas Machuca[2],
Edgar Guevara[2], Francisco Javier González[2], Juan J. Flores[1]

[1] Universidad Michoacana de San Nicolás de Hidalgo,
Facultad de Ingeniería Eléctrica,
Mexico

[2] Universidad Autónoma de San Luis Potosí,
Coordinación para la Innovación y
la Aplicación de la Ciencia y la Tecnología,
Mexico

juanf@umich.mx

Abstract. Breast cancer is one of the leading causes of death in women. Temperature measurement by means of thermography has several advantages; It is non-invasive, non-destructive and it is profitable. The measurement of breast temperature by infrared thermography is useful for detecting changes in blood perfusion that may occur due to inflammation, angiogenesis or other pathological causes. In this work, 206 thermograms of patients with suspected breast cancer were analyzed, using a classification method, in which thermal asymmetries were calculated. The most vascularized areas of each breast were extracted and compared; these two metrics were then added to obtain a thermal score, indicative of thermal anomalies. The classification method based on this thermal score allowed us to evaluate the effectiveness of the test, obtaining a sensitivity of 100%, specificity of 68.68%; a positive predictive value of 11.42% and a negative predictive value of 100%. These results highlight the potential of using infrared thermography as a complementary tool to mammography in the detection of breast cancer.

Keywords: breast cancer, infrared thermography, image analysis.

1 Introduction

Breast cancer is one of the leading causes of death in women in recent years [1, 2], affects all social levels of the population, is the first most common cancer in Mexico with 18.7%, followed by cancer of digestive organs with 18.0% [3]. The likelihood of a person developing breast cancer depends on some factors that unfortunately cannot be avoided. These include age, sex and genetics. However, there are some typical characteristics of the presence of cancer, such as tumours and specific tissue activity that specialists have been using to make an early diagnosis [4].

Studies have shown that early detection of cancer ensures a better prognosis and is essential to have a higher survival rate, if detected early, the cure rate is 95% [5].

Breast imaging techniques have been developed as primary clinical methods for the identification of early and differentiated breast cancers of benign breast tumours [6]. Mammography is the most common imaging technique used for breast cancer screening. However, the false-negative rate can reach up to 30% and exposes patients to ionizing radiation [7]. In addition, mammography is less effective in young women and in those who have dense breast tissue [8]. Ultrasound is mainly used to differentiate the properties of solid and cystic breast lesions identified by mammography. Dense breast tissue can be examined by aspiration-guided biopsy and preoperative localization. Due to the time required to perform an exam, the need for proper management training and other limitations, ultrasound alone is not suitable as a screening method for breast cancer. In fact, ultrasound and mammography can ignore many cases in which the tumour is <0.5 cm [6].

In the 1960s, infrared thermography began to be used in medical diagnosis, but until 1982 it was approved by the Food and Drug Administration (FDA) as a complementary tool for breast cancer detection [9]. Since then, the sensitivity of infrared imaging technology has increased substantially and has become a more powerful tool for the diagnosis of breast cancer [10]. The measurement of temperature through infrared thermography is advantageous since it is completely non-invasive, non-destructive, cost-effective and can provide temperature data that give a distribution over a wide area [11]. The thermal analysis of the skin's temperature distribution in order to obtain information about a possible internal tumour offers more advantages to indicate an abnormal metabolism in the early stages of cancer [12]. Therefore, thermography is very convenient for locating changes in blood perfusion that may occur due to inflammation, angiogenesis or other causes. It is known that asymmetric temperature distributions, as well as the presence of hot and cold temperature points, are good indicators of an underlying problem [13].

Although the diagnosis is usually carried out manually by experts, there is a high demand for automatic methods that can also be used as a second opinion [14]. Automated thermogram analysis consists of dividing the image into segments of interest and analyzing it later Image segmentation refers to the technique that divides a digital image into multiple sections and is generally used to identify regions of interest or other relevant information in digital images [15]. One of the main ways to differentiate anomalies in the breasts is the comparison by thermal asymmetries in which the left breast is compared with the right breast. Another important point that has been evaluated is the difference in temperature that can exist in both breasts. In this work, an effective approach to automatically analyze breast thermograms for cancer diagnosis is presented.

1.1 Interpretation of Images

The first methods of interpretation of infrared images of breast were based solely on qualitative criteria (subjective). The images were read to see the variations in the vascular pattern without taking into account the temperature variations between the breasts (Tricore method) [16]. This resulted in wide variations in the results of studies conducted with inexperienced interpreters.

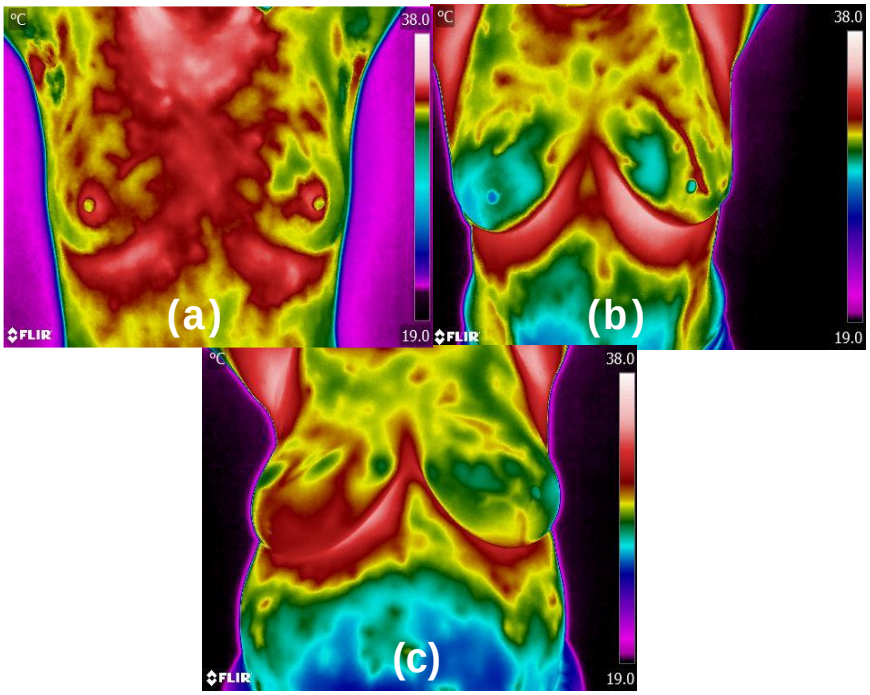

Fig. 1. Different types of vascularity (a) TH2 (normal uniform), (b) TH4 (abnormal), and (c) TH5 (severely abnormal).

Research throughout the 1970s showed that when both qualitative and quantitative data were incorporated into interpretations, an increase in sensitivity and specificity was performed. In the early 1980s, a standardized method of thermovascular analysis was proposed. The interpretation is composed of 20 discrete vascular and breast temperature attributes [17, 18].

1.1.1 Thermobiological Classification

This method of analysis was based on previous research and large-scale studies that included tens of thousands of patients. Using this methodology, thermograms are rated in one of the 5 TH (thermobiological) classifications. Based on the combined vascular pattern and temperatures across the two breasts, the images would be classified as TH1 (normal non-vascular uniform), TH2 (normal uniform vascular), TH3 (equivocal), TH4 (abnormal) or TH5 (severely abnormal) (see Fig. 1).

The use of this standardized interpretation method significantly increased the sensitivity, specificity, positive and negative predictive value of infrared images and the reliability of interpretation. The patient's continuous observations and investigations during the last two decades have caused changes in some of the thermovascular values; therefore, keeping the interpretation system updated.

Variations in this methodology have also been adopted with great success. However, it is recognized that, as with any other imaging procedure, specialized training and experience produce the highest level of success in screening.

1.1.2 Ville Marie Infrared Graduation Scale

Ths rating scale is based on relevant clinical information when comparing infrared images of both breasts and current images with previous images. An abnormal infrared image requires the presence of at least one abnormal sign (Table 1).

Table 1. Ville Marie infrared (IR) graduation scale.

Abnormal signs
1. Significant vascular asymmetry.
2. Vascular anarchy consisting of unusual tortuous or serpiginous vessels that form clusters, loops, abnormal tree planting or aberrant patterns.
3. A temperature rise of 1 ° C on the scale (DT) when compared with the contralateral site and when associated with the area of clinical abnormality.
4. A focal DT of 2 ° C against the contralateral site.
5. A focal DT of 3 ° C against the rest of the ipsilateral breast when it is not present on the contralateral side.
6. Global DT of the sinuses of 1.5 ° C against the contralateral sinus.
Infrared scale
IR1 = From the absence of any vascular pattern to mild vascular asymmetry.
IR2 = From significant but symmetrical vascular pattern to vascular asymmetry moderate, particularly if it is stable.
IR3 = An abnormal sign.
IR4 = Two abnormal signs.
IR5 = Three abnormal signs.

2 Materials and Methods

The sample consists of 206 patients from the "Dr Raymundo Abarca Alarcón" General Hospital in Chilpancingo, Guerrero, Mexico. Ages between 17 and 74 years. Average age: 42.4 years with a standard deviation of 10.4, average body mass index of 27.8 with a standard deviation of 4.8 and without dermatological diseases.

The study was presented and approved by the hospital's ethics committee. Patients invited to participate in the study had clinical evidence of a tumour suggestive of cancer, risk factors for breast cancer and went to the clinic. None of the patients had declared cancer at the time of inviting them to participate in the study, first the thermographic image was taken and then the mammogram scheduled for evaluation was performed. Patients read the informed consent form before signing it.

The specialists performed the BI-RADS classification of mammography, clinical diagnosis and biopsy were performed on those who had a suspicious anomaly in the evaluation. The camera used was the IR FlexCam Pro R, with a focal plane matrix (FPA) detector, based on vanadium oxide (VOX) uncooled microbolometer, thermal sensitivity @ 30Hz: = 0.070 ° C at 30 C, temperature range -20 ° C to 100 ° C, ± 2%

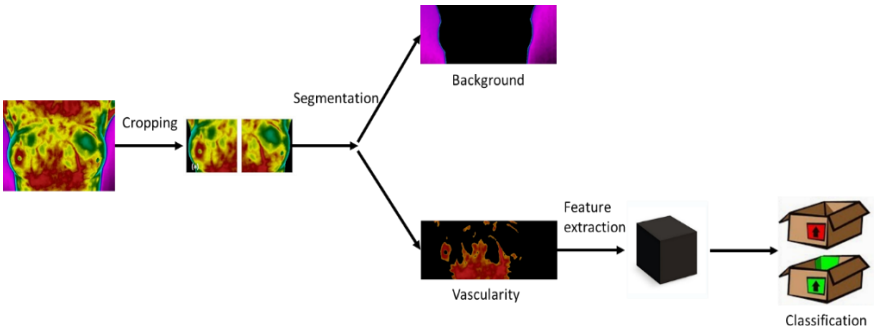

Fig. 2. Flowchart of the image processing performed.

Table 2. Scale of vascularitation.

(1) Absence of vascular patterns.
(2) Symmetric or moderate vascular patterns were found.
(3) Significant vascular asymmetry.
(4) Extended vascular asymmetry in at least one-third of the sinus area.

accuracy and a 20 mm f / 0.8 Germanium lens with a 23 ° horizontal x 17 ° vertical field of view.

The emissivity was set at 0.97 [15]. Patients who participated in the acquisition of thermal imaging did not perform physical activities, drank alcohol, smoked or used deodorant during the day the images were taken. At the time the image was taken, an acclimatization process of the patient was carried out in which they were asked to remain naked from the waist up for 20 minutes in a room with a controlled temperature of 24 ± 1 ° C.

Direct airflow to the patient was avoided and there were no nearby instruments that emit heat. The thermographic images were taken standing, with the hands holding the neck, 1.5 m from the camera, 5 photos were taken in total, one frontal, left lateral, right lateral and both frontal sinuses separately.

The automated program developed in this work is based on Gonzalez's work [10], which performs a simulation of a breast and a cancer tumor to evaluate desease through thermographic images. The interpretation of the image is done by means of a thermal score derived from the scale of the Ville Marie infrared classification [19]. This thermal score takes into account the two most significant infrared data that are: (a) the difference in surface temperature in the lesion compared to the specular imaging site in the contralateral breast (DT), and (b) the vascular pattern around and at the site of the injury [20].

The thermal score is calculated by adding the amount of vascularization to the difference in surface temperature in degrees Celsius at the site of the lesion compared to that of the contralateral breast. The amount of vascularization is determined using

the scale shown in Table 2. Fig. 2 shows the flow chart of the processing used in this work.

2.1 Left and Right Breast Segmentation

Image segmentation refers to the technique that divides a digital image into multiple segments. Segmentation is used to identify regions of interest or other relevant information in digital images [15].

The method used for the segmentation of the left and right breast from the rest of the body is based on the analysis of the projection profile [21]. It is used to find the upper, lower, left and right edges of the detected edge of the breast thermographic image. The Horizontal (or vertical) projection profile is a histogram of a matrix with a number of entries equal to the number of rows (or columns). The number of black pixels or white pixels in a row (or column) is stored in the corresponding entry.

The Horizontal Projection Profile (HPP) is used to locate the upper and lower edges. The Vertical Projection Profile (VPP) is used to find the left and right edges. First, the breast thermographic image becomes a grayscale image. Then, the following sequences of operations are performed on the image: Image filtering, edge detection, lower edge detection, upper edge detection, image threshold, left and right edge detection, central axis location, and segmentation of the left and right breast.

2.2 Edge Detection with the Sobel Operator

The Sobel operator measures the 2 D spatial gradient of the thermographic image and emphasizes the regions of high spatial frequency that correspond to the edges. The operator consists of a pair of 3 x 3 kernels to perform the convolution as shown in Eq. (4). One mask is simply the other turned 90°. These masks are designed to enhance the edges vertically and horizontally.

The Sobel operator gives a smoothing effect (average filter) and reduces false edges. In theory, the image gradient f (x, y) is a vector and is given by:

$$\nabla = \begin{bmatrix} G_x \\ G_y \end{bmatrix} = \begin{bmatrix} \frac{\partial f}{\partial x} \\ \frac{\partial f}{\partial y} \end{bmatrix}, \tag{1}$$

where ∇ is the gradient operator. The magnitude of the gradient is given by:

$$Mag(\nabla f) = \sqrt{G_x^2 + G_y^2}\,, \tag{2}$$

where Mag (∇f) gives the magnitude of the edge to a particular location x-y.

The direction of the edge is found by:

$$\alpha(x, y) = tan^{-1}\frac{G_y}{G_x}. \tag{3}$$

The coefficient matrix for the Sobel operator is defined as:

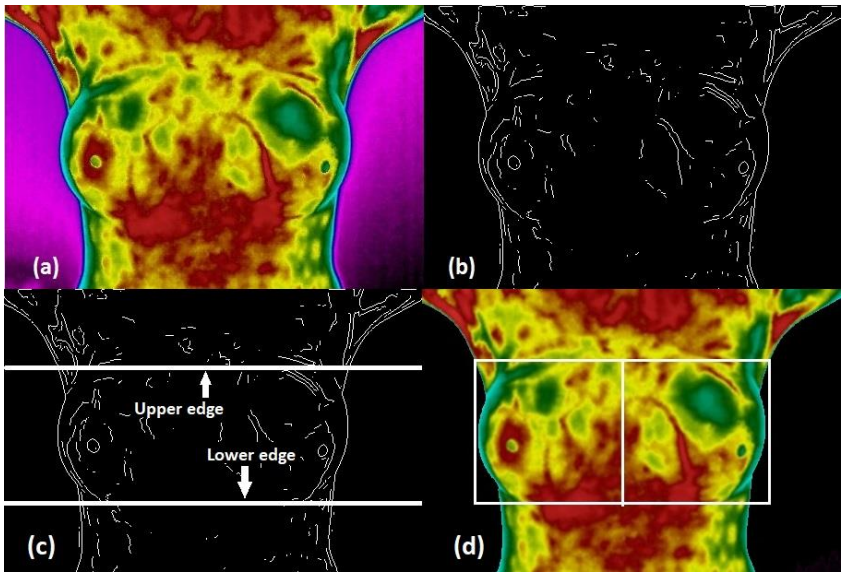

Fig. 3. Image segmentation process. (a) original image, (b) binarized image with edge detection, (c) upper and lower limits detected and (d) upper, lower, left and right edges detected.

$$H_x = \begin{bmatrix} -1 & 0 & 1 \\ -2 & 0 & 2 \\ -1 & 0 & 1 \end{bmatrix}, H_y = \begin{bmatrix} -1 & -2 & -1 \\ 0 & 0 & 2 \\ 1 & 2 & 1 \end{bmatrix}. \quad (4)$$

The filter results produce local gradient estimates for all pixels in the image in their two different directions, maintaining the following relation:

$$\nabla I(x,y) \approx \frac{1}{8}\begin{bmatrix} H_x \cdot I \\ H_y \cdot I \end{bmatrix}. \quad (5)$$

The result of the filters for each of the different senses is given by:

$$D_x(x,y) = H_x * I, D_y(x,y) = H_y * I. \quad (6)$$

Fig. 3 shows the results of edge detection of the breast thermographic image. The limit of the breast thermographic image is successfully detected using the Sobel operator as shown in Fig. 3 b).

2.3 Detection of the Upper and Lower Part of the Breasts

To find the lower breast, the edges detected in the image are scanned horizontally, to count the number of white pixels in each row of the bottom of the image.

In the infra-mammary line, the number of white pixels increases due to the infra-mammary fold of the breast. The scan is repeated until an HPP value equal to or greater than a threshold value is obtained. The HPP value will be smaller below the infra-mammary edge of the breast, as shown in Fig. 3 b). The row number corresponding to

the first high HPP value is taken as the lower limit (LL) for segmentation of the breast thermographic image.

HPP is used again to find the armpit location, which is considered as the upper end of the breast. Breast height normalization is necessary due to the variable height of the images. The breast thermographic image height varies depending on the structure and size of the breast. To standardize the height of the image, the distance between the lower edge detected and the lower part of the image is measured. The distance value varies depending on the structure and size of the breast. One study found that the distance value will be high for small breasts and less for large breasts [1]. According to the study and the observation, the height of the breast is calculated as indicated below.

1. If the distance between the bottom of the image and the lower limit of the breast is less than 26.3%[1] total pixels of the height then:

$$h = \frac{1}{2}m\,, \tag{7}$$

where h is the height of the area of interest of the image and m is the total number of rows present in the image.

2. If the distance between the bottom of the image and the lower limit of the breast is greater than 26.3% total pixels of the height then:

$$h = \frac{5}{6}m\,. \tag{8}$$

3. The upper limit (LS) shall be located in the row position given by:

$$LS = LI - h\,. \tag{9}$$

Finally, the upper and lower limits detected are shown in Fig. 3 (c). Horizontal lines along the upper and lower limits were drawn in the images to illustrate the process, but they do not represent real data.

2.4 Right and Left Edge Detection

After the thermographic image of the breast is segmented from the unwanted upper and lower part, the left and right edges are detected from the image using the vertical projection profile (PPV) method. This algorithm (PPV) is defined as the white pixel count number for each column. The steps followed for the detection of the left border are given below:

1. Segment the image with the upper and lower edges and apply Sobel.

2. To find the left limit, the image is analyzed from right to left and, if a white pixel is found, the position of the last column where it was found is stored, pointing only to the left-most white pixel.

[1] This percentage was determined empiricaly to capture and crop the breast area [13].

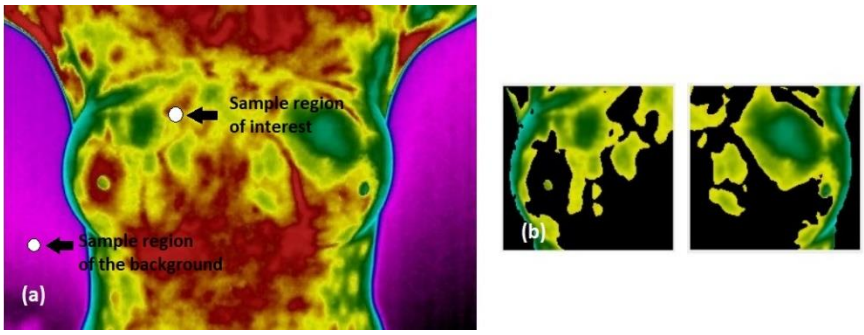

Fig. 4. Vascular areas segmentation. (a) Regions samples used to find the vascularity and eliminate the background in the images and (b) Segmented sinuses with vascularized area removed.

3. To find the right limit, the image is analyzed from left to right and, if a white pixel is found, the position of the last column where it was found is stored, pointing only to the white pixel farthest to the right. Therefore, the left and right edges detected are used to form a thermographic image of the desired breast by removing the unwanted left and right parts. In addition, the central axis of the breast is determined by dividing the width of the new image divided by two. Finally, Fig. 3(d) shows a thermographic image of the breast with the edges highlighted at the bottom, top, left and right.

2.5 Thermal Vascularity

An important part of image processing is the calculation of thermal vascularization. This process is performed in the color space known as CIELAB, which is normally used to describe all the colors that the human eye can perceive. In fact, it is done by removing the reddest parts of the image.

Fig. 3 (d) shows the areas with the highest temperature. The color space L * a * b * (also known as CIELAB or CIE L * a * b *) allows quantification of visual differences. In this color model, space is defined by three variables: L * represents brightness, and a * and b * correspond to the hue components. a * defines the distance along the red-green axis, and b * along the blue-yellow axis, these axes define the CIEXYZ space [22].

During the calculation of thermal vascularization, first, an image in the RGB space is converted to the L * a * b * space. Then, two sample regions of interest are selected; one in the vascular area and one in the background. We obtain the average a * b * of the selected areas, as shown in Figure 3.4 a). These values serve as markers for space a * and b * of background and vascular pixels. Next, each pixel is classified by calculating the Euclidean distance between that pixel and the marker. If that distance is too small, the pixel will be labelled as the closest marker. The result is a binary array that indicates each pixel's class.

Subsequently, the masks created in the background and red regions are used to segment the image by color, as well as to find vascularization. Once the original image is segmented by colors, the same values (upper, lower, left, right, and center) are used to separate the contours of the breasts and vascularized areas in order to calculate the

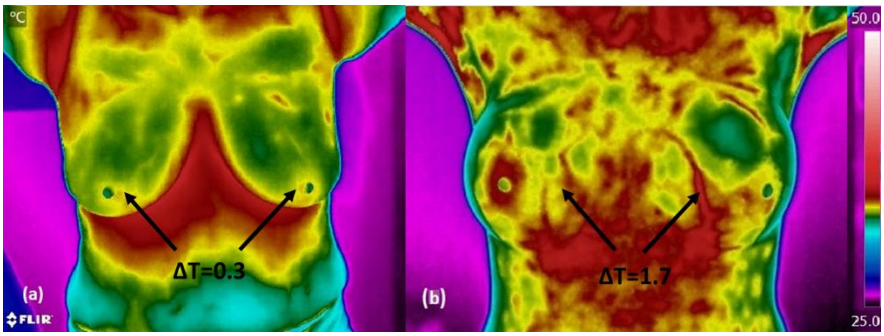

Fig. 5. Cancer diagnosis process. (a) IR image of healthy breasts. (DT) represents the difference in the surface of the breast. The calculated thermal score was found to be 1.3, obtained by adding the amount of vascularity (1): Absence of vascular patterns, while a value of 0.3 corresponds to the difference in surface temperature, DT, at the location of the lesion, compared to the contralateral breast and (b) IR image of a patient with infiltrating ductal carcinoma. The calculated thermal score was assigned to 3.7, obtained by adding the amount of vascularity (2): the two values denote symmetrical or moderate vascular patterns and a value of 1.7, associated with the surface temperature difference, DT, at the site of the lesion compared to the contralateral breast.

thermal score (Fig. 4 b). Subsequently, values from 1 to 4 are assigned according to the scale shown in Table 2.

Finally, the temperature difference of the heat source located in one of the breasts is measured with respect to its contralateral part. This is done with the thermal camera in real-time, that is, taking the images, observing them in one breast and then in their counterpart to obtain the temperature difference of interest. Then, a delta temperature is added to the thermal score (with a value of 2) of the vascularization found above, as shown in Fig. 5 b).

3 Results

All patients with a BI-RADS indicating the possibility of cancer underwent a biopsy. Of those patients, 8 of them exhibited infiltrating ductal carcinoma. Thermograms were analyzed using thermal scoring as presented in the previous section. Here, the infrared images were divided into two groups, (1) those with a thermal score below 2.5 were classified as healthy, (2) those with a thermal score greater than or equal to 2.5 were classified with some anomaly. Once the classification is performed on all images, a final score is assigned to the corresponding thermal image, for example, Fig. 3.5 b) shows a cancer patient with a thermal score of 6.7.

Further analysis of the thermographic images reveals statistical data as follows: of 206 patients, 8 true positives and 62 false positives were found. In addition, 136 were classified as true negatives and there were no false negatives. Obtaining a sensitivity of 100% with a specificity of 68.68%, a positive predictive value of 11.42%, and a negative predictive value of 100%. Fig. 6 shows the receiver operating characteristics (ROC) curve of thermographic analyses using the automated program. Based on the results, the ROC curve allows us to infer that it is possible to increase the specificity

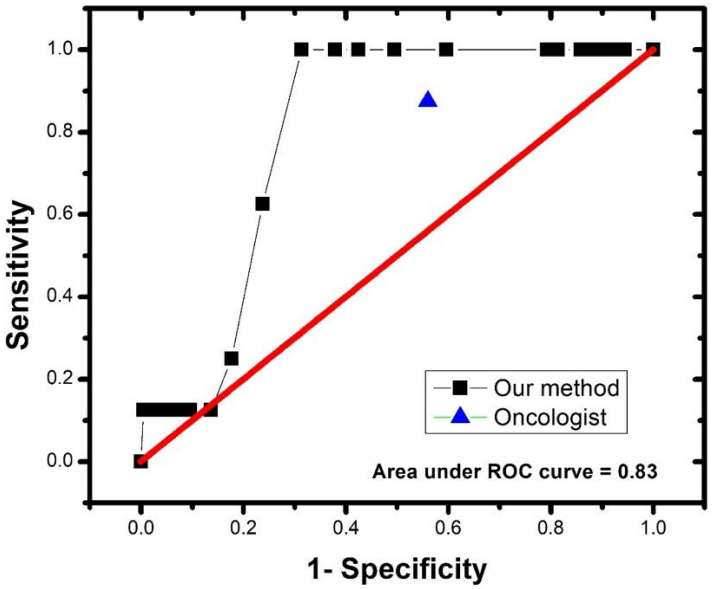

Fig. 6. ROC curve of the automated thermogram classification program.

Table 3. Comparison between our automated method and qualitative evaluation by an oncologist expert in thermography.

	Oncologist	**Our program**
Total of patients	206	206
Sick patients	8	8
Healthy patients	198	198
True positive	7	8
False positives	87	62
True negatives	111	136
False negatives	1	0
Sensitivity	87.50%	100%
Specificity	56.06%	68.68%
VPP	7.44%	11.42%
VPN	99.10%	100%

with this method by moving the cut-off point of the test, otherwise, the sensitivity would decrease considerably.

It is worth mentioning that the same thermographic images were analyzed qualitatively by an oncologist in a double-blind study, their findings were 7 true positives and 87 false positives, while 111 were classified as true negative and 1 false negative. The comparison of the results of the qualitative and quantitative method with our method is shown in Table 3.

4 Conclusions

A classification of thermographic images for the detection of breast cancer was performed using an automated program. 206 patients were considered for the screening test with clinical evidence of a tumour risk factor for breast cancer, the BI-RADS classification of mammography, the clinical diagnosis and the pathological results of the biopsy. The analyzed thermograms were classified as healthy (<2.5 thermal scores) or with an anomaly (≥2.5 thermal scores). The findings revealed that patients classified as healthy really had a healthy state (automated program) with a sensitivity of 100% and a specificity of 68.68%. In contrast, the same images qualitatively analyzed by an expert showed a sensitivity of around 87.5% and a specificity at 56%, so our results showed a significant improvement over a manual procedure.

In addition, an automated method to analyze thermograms was implemented, increasing the sensitivity and specificity of the test under study. The main objective will be to help the experts helping them with a better detection tool or even providing the possibility that someone without experience can benefit from the test results. We can emphasize that infrared thermography is not intended to replace mammography, but it is an excellent primary method/technique before patients undergo X-rays. It could be considered as a complementary diagnostic method to improve breast cancer detection.

Mamographies are an invasive and painful procedure. The proposed method is not intended to replace mamographies, but to avoid the suffering of undergoing one when it is absolutely not necessary. Using the proposed methodology, a mammography can be applied only those patients whose thermographic analysis indicates a breast abnormality.

References

1. Rastghalam, R., Pourghassem, H.: Breast cancer detection using MRF-based probable texture feature and decision-level fusion-based classification using HMM on thermography images. Pattern Recognition, 51, pp. 176–186 (2016)
2. González, F.: Thermal simulation of breast tumours. Revista Mexicana de Física, 53(4), pp. 323–326 (2007)
3. INEGI: Instituto Nacional de Estadística y Geografía (2015)
4. Guzman-Cabrera, R., Guzman-Sepulveda, J.R., Parada, A.G., Garcia, J.R., Cisneros, M.T., Baleanu, D.: Digital processing of thermographic images for medical applications. Revista De Chimie, 67(1), pp. 53–56 (2016)
5. Gautherie, M.: Thermopathology of breast cancer: measurement and analysis. Annals of the New York Academy of Sciences, pp. 383–415 (1980)
6. Yao, X., Wei, W., Li, J., Wang, L., Xu, Z.L., Wan, Y., Li, K., Sun, S.: A comparison of mammography, ultrasonography, and far-infrared thermography with pathological results in screening and early diagnosis of breast cancer. Asian Biomedicine, 8(1), pp. 11–19 (2014)
7. Boquete, L., Ortega, S., Miguel-Jiménez, J.M., Rodríguez-Ascaris, J.M., Blanco, R.: Automated detection of breast cancer in thermal infrared images, based on independent component analysis. Journal of Medical Systems, 36(1), pp. 103–111 (2012)
8. Wishart, G.C., Campisi, M., Boswell, M., Chapman, D., Shackleton, V., Iddles, S., Hallett, A., Britton, P.D.: The accuracy of digital infrared imaging for breast cancer detection in

women undergoing breast biopsy. European Journal of Surgical Oncology, 36(6), pp. 535–540 (2010)
9. Arora, N., Martins, D., Ruggerio, D., Tousimis, E., Swistel, A.J., Osborne, M.P., Simmons, R.M.: Effectiveness of a noninvasive digital infrared thermal imaging system in the detection of breast cancer. American Journal of Surgery, 196(4), pp. 523–526 (2008)
10. González, F.J.: Non-invasive estimation of the metabolic heat production of breast tumours using digital infrared imaging. Quantitative InfraRed Thermography Journal, 8(2), pp. 139–148 (2011)
11. Han, F., Shi, G., Liang, C., Wang, L., Li, K.: A simple and efficient method for breast cancer diagnosis based on infrared thermal imaging. Cell Biochemistry and Biophysics, 71(1), pp. 491–498 (2014)
12. Kathryn, J.C., Sireesha, G.V., Stanley, L.: Triple negative breast cancer cell lines: One tool in the search for better treatment of triple negative breast cancer. Breast Dis, 32, pp. 35–48 (2012)
13. Schaefer, G.: ACO classification of thermogram symmetry features for breast cancer diagnosis. Memetic Computing, 6(3), pp. 207–212 (2014)
14. Krawczyk, B., Schaefer, G.: A hybrid classifier committee for analysing asymmetry features in breast thermograms. Applied Soft Computing Journal, 20, pp. 112–118 (2014)
15. Zhang, X., Li, X., Feng, Y.: A medical image segmentation algorithm based on bi-directional region growing. Optik, 126(20), pp. 2398–2404 (2015)
16. Gauthrie, M., Kotewicz, A., Gueblez, P.: Accurate and objective evaluation of breast thermograms: basic principles and new advances with special reference to an improved computer-assisted scoring system. Thermal Assessment of Breast Health, pp. 72–93 (1983)
17. Hobbins, W.B.: Abnormal thermogram—significance in breast cancer. Interamer. J. Rad, 12, pp. 337 (1987)
18. Gautherie, M.: New protocol for the evaluation of breast thermograms. Thermological Methods, pp. 227–235 (1985)
19. Keyserlingk, J.R., Ahlgren, P.D., Yu, E., Belliveau, N.: Infrared imaging of the breast: initial reappraisal using high-resolution digital technology in 100 successive cases of stage i and ii breast cancer. pp. 245–251 (1998)
20. Wang, J., Chang, K.J., Chen, C.Y., Chien, K.L., Tsai, Y.S., Wu, Y.M., Teng, Y.C., Shih, T.: Evaluation of the diagnostic performance of infrared imaging of the breast: a preliminary study. BioMedical Engineering OnLine, 9(1), pp. 3 (2010)
21. Dayakshini, D., Kamath, S., Prasad, K., Rajagopal, K.V.: Segmentation of breast thermogram images for the detection of breast cancer – a projection profile approach. Journal of Image and Graphics, 3(1), pp. 47–51 (2015)
22. Cuevas, E., Zaldívar, D., Pérez, M.: Procesamiento digital de imágenes con MATLAB & Simulink. Ra-Ma (2016)